Cell Proliferation

Cell Prolif., 2010, **43**, 372–377 doi: 10.1111/j.1365-2184.2010.00686.x

Spontaneous immortalization of neural crest-derived corneal progenitor cells after chromosomal aberration

C. Brandl*, J. Kaesbauer†, B. H. F. Weber* and C. Morsczeck‡

**Institute of Human Genetics, University of Regensburg, Regensburg, Germany, †Centre for Human Genetics, Regensburg, Germany, and ‡Department of Conservative Dentistry and Periodontology, University of Regensburg, Regensburg, Germany*

Received 20 *August* 2009; *revision accepted* 4 *November* 2009

Abstract

Objectives: In a previous study, we have reported the existence of neural crest-derived stem cell-like cells originating from the corneal limbus of juvenile mice (termed murine corneal cells, MCCs). To yield a sufficient number of MCCs, for example, for cell-therapy approaches, here we have investigated MCCs' ability for extensive proliferation, and we have evaluated their stem cell qualities and genetic stability after large-scale culture.

Materials and methods: MCCs were established from corneal limbal tissue of juvenile mice. To determine their cell proliferation and self-renewing potential, MTT tests and an estimation of colony forming unit efficiency were carried out. Multipotency of cell differentiation was examined by applying adipogenic and osteogenic differentiation protocols. Moreover, karyotyping was performed and expression of stem cell markers and cell cycle-associated genes was analysed.

Results: MCCs, as primary cells, could be cultured for more than 60 passages. We observed increased cell proliferation and high number of colony forming units (CFUs) after extensive culture. Interestingly, there were no changes in expression of MCC markers. Furthermore, cell differentiation potentials remained comparable with MCCs at early passages. However, karyotyping revealed numeric chromosomal aberrations at higher passages. Moreover, tumour suppressor genes such as *p16* and *p21* were found to be down-regulated after large-scale cell culture.

Conclusions: MCCs immortalize spontaneously after extensive cell culture, but still demonstrate stem cell-like qualities.

Correspondence: C. Morsczeck, Department of Conservative Dentistry and Periodontology, University of Regensburg, Franz-Josef-Strauß-Allee 11, 93053 Regensburg, Germany. Tel.: +49(0)941 9446161; Fax: +49(0)941 9446025; E-mail: christian.morsczeck@klinik.uni-regensburg.de

Introduction

As the outermost surface of the eye, the cornea not only functions as a strong protective shield against external insults, but also provides optical function by transmitting and focusing light on the retina. It is comprised of three structurally unique and highly specialized cell layers – the epithelium, stroma and endothelium – whose homeostasis, deturgescence and integrity are essential for visual acuity. These layers are constituted of several different cell types including epithelia, endothelial cells and keratocytes, the last shaping the corneal stroma (1–4).

Among these heterogeneous corneal cell populations, which all provide the cornea with its essential character, different types of stem or progenitor cells have been identified and the cornea has become of interest as an area of stem cell research (3–9). Stem cells have proven to be an intriguing source of tissues for use in cell-based therapy and corneal tissue engineering. Keratoplasty, currently the only effective method of providing recovery of vision after corneal blindness, raises many problems and there is significant interest in alternatives. Stem cells are promising tools for new therapeutic strategies, but to properly exploit the recent advances of corneal stem cell research, many questions remain to be answered (4,10).

In a previous study, we have identified a neural crest-derived corneal stem-like cell population (named murine corneal cells, MCCs). MCCs originate from the corneal limbus of juvenile mice before the stage of eyelid opening. They express a unique marker profile including typical neural crest-originated stem cell transcripts such as Sca1 and other stem/progenitor cell markers such as Notch1, Nes, Abcg2 and Cd34. MCCs have further prove stem cell-like attributes, such as cell migration, proliferation

and, most interestingly, multipotency under *in vitro* conditions after differentiation into cells with features resembling adipocytes, osteoblasts and neuronal cells (11).

To use MCCs in cell-based therapies of corneal tissue, high cell numbers are recommended. MCCs are somatic stem-like cells and have a limited lifespan that generally restricts their value for cell-based therapies. In our previous study, we observed a significant decrease in cell proliferation during the first cell passages although our investigations were conducted up to passage 10 (11). In the present study, we have focused on MCCs at later passages and investigated to what extent their sub-culture would be possible and whether they maintain their stem cell-like qualities and genetic stability after extensive proliferation.

Materials and methods

Isolation and cell culture

The MCCs were established from wild-type C57Bl6/J mice purchased from Charles River Laboratories (Wilmington, MA, USA). All animals were housed and handled in full accordance with institutional guidelines and killed at maximum 8 days of age. Cells were isolated as described previously (11). In brief, discs of whole corneas including the limbal area of at least five eyes were chopped into fine pieces, rinsed and collected in PBS (PAA, Pasching, Austria). After being centrifuged at 800 ***g*** for 2 min, tissue pellets were resuspended in growth medium, high-glucose DMEM (4.5 g/l of glucose) with L-glutamine (PAA), supplemented with 10% foetal bovine serum (PAA) and 1x penicillin/ streptomycin (PAA). Tissue pieces were subsequently seeded in 25 cm^2 culture flasks (Nunc, Denmark); they attached to culture dish surface and after 3–5 days, an exodus of single cells could be observed. Cultures were maintained in humidified air (5% CO_2) at 37 °C and medium was changed twice a week. Upon reaching confluence, cells were detached using trypsin–EDTA (PAA) and again subcultured in growth medium, being plated at initial densities of 5–8 $\times$ 10^3 cell/cm^2.

Colony-forming unit assay

For measurement of colony-forming units (CFUs), MCCs were plated in six-well tissue culture plates (BD-Falcon, Bedford, MA, USA) at initial density of 1 $\times$ 10^3 cells/well and cultured in growth medium for 10 days. For better observation, CFUs appearing were stained with crystal violet ACS reagent (Sigma-Aldrich, Taufkirchen, Germany). Colonies above 50 cells were counted using phase contrast microscopy (Nikon Eclipse TE 2000-S; Nikon, Düsseldorf, Germany).

MTT assay

To investigate cell proliferation, MTT assays were performed. MCCs were seeded in six-well tissue culture plates (Falcon) containing growth medium, at initial density of 5000 cells/cm^2 and were incubated for 72 h. Growth medium was then replaced with fresh medium containing 10% 3-[4,5-Dimethylthiazol-2-yl]-2,5-diphenyltetrazoliumbromide (MTT) solution (Sigma-Aldrich). After incubating for 4 h at 37 °C in 5% CO_2, dark purple formazon crystals formed were dissolved in 0.1 N HCl (Roth, Eggenstein-Leopoldshafen Germany) in anhydrous isopropanol (Roth). This solution was subsequently measured photometrically at a wavelength of 540 nm (Ultrospec 2100pro; Amersham Biosciences, Buckinghamshire, UK).

Reverse transcription-polymerase chain reaction

To analyse gene expression, total RNA was isolated from cultured cells using the NucleoSpin RNA II kit (Macherey-Nagel, Düren Germany) including on-column DNAse digestion according to manufacturer's recommendation. RNA was quantified using a NanoDrop ND-1000 Spectrophotometer (Thermo, Wilmington, DE, USA) and RNA quality was controlled by Agilent 2100 Bioanalyzer (Agilent, Wilmington, DE, USA). First-strand cDNAs were synthesized according to instructions of the RevertAid H Minus First Strand cDNA Synthesis Kit (Fermentas, St. Leon-Rot, Germany). PCR was performed using GoTaq Green Master Mix Kit (Promega, Mannheim, USA) at final volume of 20 µl and Thermocycler T3000 (Biometra, Göttingen Germany). Gene-specific primers are provided in Table 1. PCR products were electrophoretically separated in 1.5% agarose gel. All genes were amplified for 35 cycles, whereas glyceraldehyde-3-phosphate dehydrogenase (Gapdh), which served as a housekeeping gene, was amplified for only 25 cycles.

Quantification of mRNA expression for cell cycle-associated genes was performed by real-time quantitative RT-PCR (qRT-PCR), using 7900HT Fast Real-Time PCR System (Life Technologies, Applied Biosystems, Carlsbad, CA, USA). Gene-specific primers are provided in Table 2. Relative differences in gene expression were calculated after normalization based on *glucuronidase beta (Gusb)* expression and were analysed using the $\Delta\Delta$CT method (12).

Adipogenic and osteogenic differentiation

To initiate adipogenic and osteogenic differentiation *in vitro*, the MCCs were plated in six-well tissue culture plates (BD-Falcon) at initial density of 5000 cells/cm^2 and grown to subconfluence in normal growth medium.

Table 1. Gene-specific primers for RT-PCR

Gene	Primer sequence (5′-3′)	Product size (bp)	GenBank accession ID
Notch1	Forward: TGCCTGTGCACACCATCCTGC Reverse: CAATCAGAGATGTTGGAATGC	247	NM_008714
Nes	Forward: AATGGGAGGATGGAGAATGGAC Reverse: TAGACAGGCAGGGCTAAGCAAG	496	NM_016701
Abcg2	Forward: CCATAGCCACAGGCCAAAGT Reverse: GGGCCACATGATTCTTCCAC	327	NM_011920
Musahi1	Forward: GGCTTCGTCACTTTCATGGACC Reverse: GGGAACTGGTAGGTGTAACCAG	542	NM_008629
Twist	Forward: CCAGAGAAGGAGAAAATGGACAGTC Reverse: AAAAAGTGGGGTGGGGGGACACAAA	259	NM_011658
Snail	Forward: CCCACTCGGATGTGAAGAGATACC Reverse: ATGTGTCCAGTAACCACCCTGCTG	534	NM_011427
Lum	Forward: TGCTGTCTCGGCTTCTCTGAAAG Reverse: AACATCCCCCACATTCCCAACC	567	NM_008524
Vim	Forward: ATGCTTCTCTGGCACGTCTT Reverse: AGCCACGCTTTCATACTGCT	206	NM_011701
Ki67	Forward: GAGCAGTTACAGGGAACCGAAG Reverse: CCTACTTTGGGTGAAGAGGCTG	262	X82786
Gapdh	Forward: GACCACAGTCCATGCCATCAC Reverse: TCCACCACCCTGTTGCTGTAG	453	NM_008084

Table 2. Gene-specific primers for qRT-PCR

Gene	Primer sequence (5′-3′)	Probe ID[a]	GenBank accession ID
Tert	Forward: agagctttgggcagaagga Reverse: gagcatgctgaagagagtcttg	107	NM_009354
p16	Forward: cgacgggcatagcttcag Reverse: gctctgctcttgggattgg	81	NM_001040654
p21	Forward: tccacagcgatatccagaca Reverse: ggacatcaccaggattggac	21	NM_007669
Gusb	Forward: gtgggcattgtgctacctc Reverse: atttttgtcccggcgaac	25	NM_010368

[a]Probe number from Roche Universal Probe Library.

Subsequently, cells were switched to differentiation media and those left in growth medium were used as controls. Media were changed twice a week.

Adipogenic differentiation was performed in DMEM High glucose (4.5 g/l) with L-glutamine (PAA), 10% FBS (PAA), 1x penicillin/streptomycin (PAA), 100 nM dexamethasone (Sigma-Aldrich), 0.5 mM 3-isobutyl-1-methylxanthine (Sigma-Aldrich) and 10 µg/ml h-insulin (Sigma-Aldrich). Cell cultures were maintained for 14 days and finally analysed using oil red O staining.

For osteogenic differentiation, MCCs were cultured in DMEM high glucose (4.5 g/l) with L-glutamine (PAA) containing 10% FBS (PAA), 1x penicillin/streptomycin (PAA), 0.1 µM dexamethasone (Sigma-Aldrich), 100 µM L-ascorbic acid 2-phosphate (Sigma-Aldrich), 2.9 mM KH_2PO_4 (Sigma-Aldrich) and 20 mM Hepes (PAA). The experiment was conducted for 28 days and subsequently analysed using alizarin red staining.

Chromosome preparation

For numerical and structural chromosomal analyses of MCCs, karyotyping was performed. They were grown to subconfluence as a monolayer in culture flasks (Nunc, Roskilde, Denmark) in normal growth medium. Cells were then synchronized using thymidine solution (Sigma-Aldrich) and subsequently treated with colcemid (Roche, Mannheim, Germany) for 120 min at 37 °C. After being detached from surfaces using trypsin–EDTA (PAA), cells were centrifuged. The cell pellet was resuspended and maintained in hypotonic solution (75 mM KCl) for 20 min at 37 °C, centrifuged again and finally fixed in methanol

and acetic acid. Metaphase spreads were prepared on coverslips (Roth), dried overnight and Giemsa stained after trypsin pre-treatment.

Results

MCCs surprisingly, could be grown for more than 60 passages and their proliferation levels increased even after passage 10 (Fig. 1). To estimate their self-renewing potential at higher passages, CFU efficiencies were determined. Previous results revealed 22.3 ± 1.97 CFUs per 1000 cells in passage 2, which decreased significantly to 2.0 ± 0.58 CFUs per 1000 cells in passage 7 (11). New measurements using the same cell line demonstrate another significant increase to 62.2 ± 1.77 CFUs per 1000 cells in passage 57 ($P < 10^{-10}$). Interestingly, no significant changes in morphology or size of colonies were observed during cell culture (data not shown).

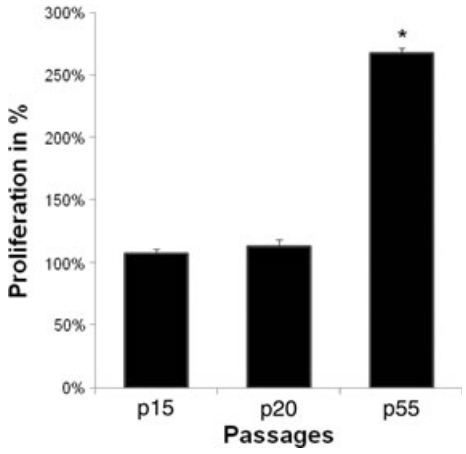

Figure 1. Proliferation of MCCs in late passages. Proliferative capacity was measured at passages 15, 20 and 55. At passage 5, proliferation as determined in previous studies was set as 100%. Each bar represents average ± standard deviation of six biological replicates (*Student's *t*-test: $P < 0.0000000001$).

To examine eventual changes in gene expression profile of MCCs during cell culture, characteristic markers were compared at early and late passages (Fig. 2). These markers were determined in a previous study (11). Intriguingly, stem/progenitor cell markers such as *Notch gene homolog 1 (Notch1), nestin* (*Nes), ATP-binding cassette subfamily G member 2* (*Abcg2*) and *Musashi homolog 1* (*Musahi 1*) were found at both passage 3 and passage 15. Neural crest markers *twist gene homolog 1 (Twist)* and *snail homolog 1 (Snail)* as well as markers associated with corneal stromal keratocytes such as *lumican* (*Lum*) and mesenchymal cell marker *vimentin* (*Vim*) were also detectable in both passage 3 and passage 15. Moreover, results indicate that expression of cell proliferation marker antigen, identified by monoclonal antibody Ki 67, (Ki67) might have been increased in passage 15.

For further exploration of stem cell qualities of MCCs after extensive culture, the potential of cell differentiation was investigated by applying adipogenic and osteogenic differentiation protocols. Results show that these MCCs were capable of adipogenic and osteogenic differentiation, at both early and late passages (Fig. 3).

To evaluate genetic stability of the cells, chromosomal analyses were performed at both early and late passages. Karyotyping revealed that they had numerical and structurally normal karyograms of 40 chromosomes at passage 8 (Fig. 4). At passage 25, the cells no longer showed diploid chromosome complements but revealed huge numerical aberrations. Forty investigated metaphases demonstrated average of 87.8 ± 31.97 chromosomes per cell. At passage 55, 40 investigated metaphases demonstrated average of 70.6 ± 9.47 chromosomes per cell.

Expression of important cell cycle-associated genes of early and late passages was analysed by qRT-PCR measurements (Fig. 5). Interestingly, *telomerase reverse transcriptase* (*Tert*) was significantly down-regulated after large-scale proliferation. Moreover, tumour suppressor genes *cyclin-dependent kinase inhibitor 2A* (*p16)* and

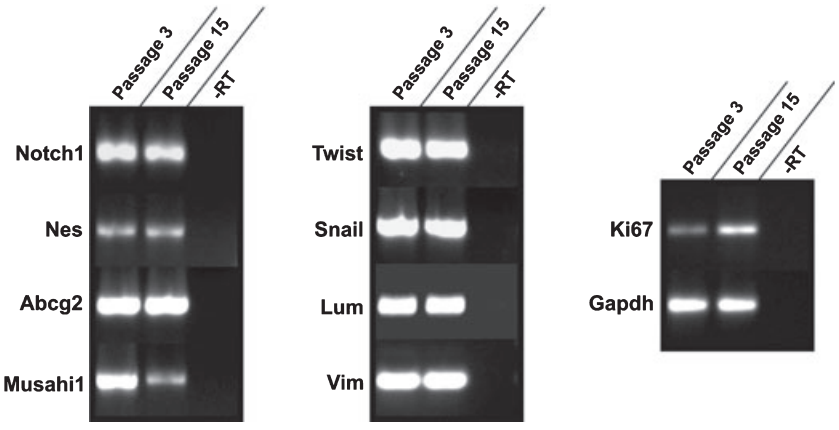

Figure 2. RT-PCR of MCCs at early and late passages. Total RNA was isolated at passage 3 and 15. RT-PCR was performed with gene-specific primers and analysed by agarose gel electrophoresis on a 1.5% gel. *Gapdh* was used as housekeeping gene. −RT = total RNA of MCCs without reverse transcriptase (negative control).

cyclin-dependent kinase inhibitor 1A (*p21*) also significantly decreased during the process of cell culture.

Discussion

Previously, we have reported isolation of neural crest-derived cells originating from the corneal limbus of juvenile mice. These MCCs demonstrate stem cell-like features, such as cell migration, proliferation, clonogenicity and multipotency, and they express stem or progenitor cell markers such as Sca1, Notch1 and Nes. Moreover, we have found that both cell proliferation and CFU efficiencies of the cells decline remarkably up to passage 10 (11).

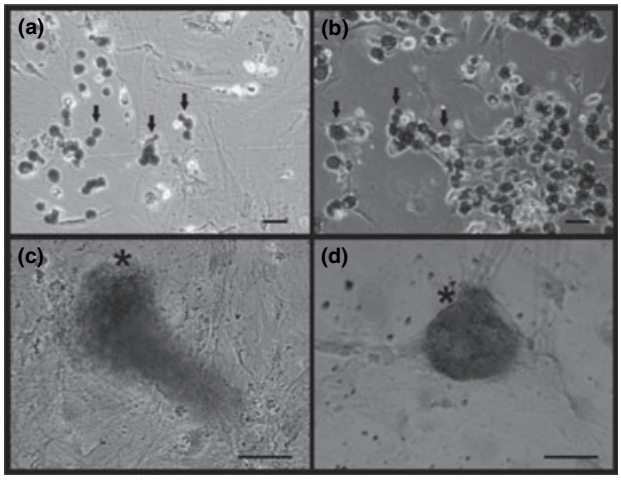

Figure 3. Adipogenic and osteogenic differentiation of MCCs at early and late passages. (a) MCCs at passage 4 revealed many lipid droplets (arrows) after being subjected to the adipogenic differentiation protocol. Cells were stained with oil red O. (b) MCCs at passage 24 also stained positively for lipid droplets (arrows). (c) At passage 4 cells revealed calcium accumulations (asterisk) after being subjected to the osteogenic differentiation protocol. These were stained with alizarin red. (d) Cells at passage 24 also stained positively for calcium accumulation (asterisk). Scale bars: 50 μm.

In the present study, we have successfully subcultured MCCs beyond passage 10. They showed lifespan of at least 60 passages, which is unusual for primary somatic cells. Generally, the utility of primary cells is limited by their restricted lifetime (13). Nevertheless, for cell-based therapy approaches of corneal tissue, MCCs should be present in high cell numbers. In addition, proliferation and CFU capacity demonstrated marked increase in the cells, outmatching passage 10, although applying identical cell culture techniques were used.

Intriguingly, MCCs upheld their characteristic gene expression profile, including stem/progenitor cell markers. Moreover, they maintained their multipotency during cell culture and even after late passages still differentiated into cells with features resembling adipocytes and osteoblasts.

However, our findings demonstrate that the MCCs acquired numerical chromosomal aberrations during cell culture, ranging from normal diploid chromosome number at early passages to more than tetraploid at later passages. It is known that aneuploidy is very frequently present in cells of solid tumours, and that tumour cells become increasingly aneuploid with tumour progression (14). Interestingly, decrease in chromosomes was observed between passages 25 and 55 for reasons unknown.

Additionally we analysed cell cycle-associated genes, *Tert, p16* and *p21*, which are often regulated in immortalized tumour cells. Results demonstrated that *Tert* was significantly down-regulated in late passages. It is widely known that telomerase expression plays a substantial role in cell senescence, as it is normally repressed in postnatal somatic cells, resulting in progressive shortening of telomeres. Deregulation of telomerase expression in somatic cells may be involved in oncogenesis. Interestingly, studies in mice suggest that telomerase also participates in chromosomal repair (15–17). Furthermore, expression of *p16* decreased as well in late passages. *p16* is known to be an important tumour suppressor gene in

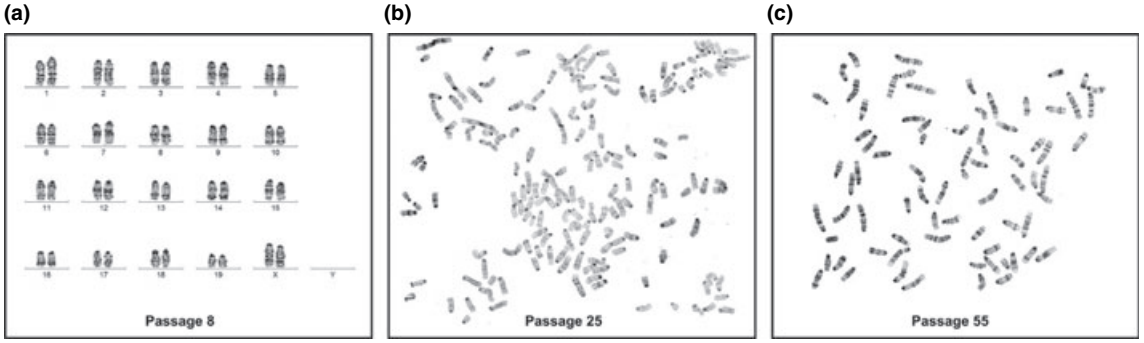

Figure 4. Karyotyping of MCCs at early and late passages. (a) MCCs at passage 8 revealed a numerical and structurally normal diploid karyogram of 40 chromosomes. (b) In contrast, at passage 25 they demonstrated huge numerical chromosomal aberrations. The given example displays 168 chromosomes found in a single cell. (c) Cells at passage 55 again revealed numerical chromosomal aberrations. The given example shows a nearly tetraploid complement of 76 chromosomes.

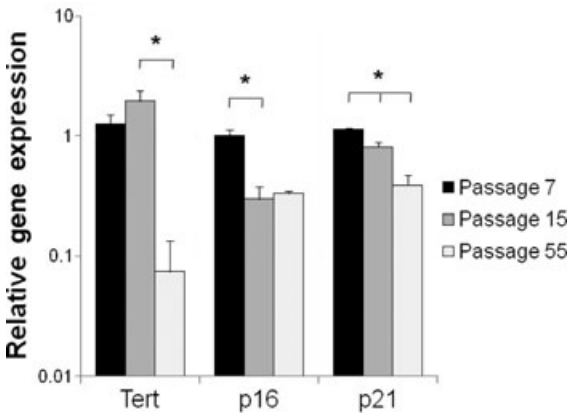

Figure 5. qRT-PCR analysis of cell cycle-associated genes in MCCs at early and late passages. Total RNA was isolated from the cells at passages 7, 15 and 55. qRT-PCR was performed with gene-specific primers for *Tert, p16* and *p21*. *Gusb* was used as housekeeping gene. Each bar represents average ± standard deviation of three biological replicates (*Student's *t*-test: $P < 0.005$).

mice (as in other species), and it frequently mutated or deleted in a wide variety of tumours. Increased expression of *p16* usually reduces proliferation of stem cells and increases cell senescence (18,19). However, we found the cell cycle inhibitor *p21* to be down-regulated. *p21* plays a major role in DNA damage response and is also implicated in terminal differentiation and replicative senescence. It has additionally been shown that *p21* knockout mice spontaneously develop tumours, which clearly shows the importance of *p21* in tumour suppression (20–22). Considering these observations, we have drawn the conclusion that MCCs after extensive proliferation develop features resembling tumourigenic cells.

This study reports successful sub-culture of MCCs up to at least until passage 60. At higher passages they retain expression of stem/progenitor cell markers and maintain stem cell-like properties such as proliferation, clonogenicity and multipotency of differentiation. However, karyotyping of MCCs at higher passages revealed numerical chromosomal aberrations. Beside this, down-regulation of tumour suppressor genes such as *p16* and *p21* underlined our assumption that these stem cell-like cells underwent transformation and resembled tumourigenic cells during long-term culture. This transformation might have taken place after passage 10 but before passage 15. Therefore, utility of MCCs for therapeutic applications might be limited and clearly restricted to those not older than passage 10, where their genetic stability has been assured. Nevertheless, establishing a novel, stable and well-proliferating stem-like corneal cell line, which maintains its multipotency of cell differentiation, should allow and facilitate further studies on corneal cell biology or stem cell biology.

References

1 Castro-Munozledo F (2008) Corneal epithelial cell cultures as a tool for research, drug screening and testing. *Exp. Eye Res.* **86**, 459–469.
2 West-Mays JA, Dwivedi DJ (2006) The keratocyte: corneal stromal cell with variable repair phenotypes. *Int. J. Biochem. Cell Biol.* **38**, 1625–1631.
3 Yoshida S, Shimmura S, Nagoshi N, Fukuda K, Matsuzaki Y, Okano H *et al.* (2006) Isolation of multipotent neural crest-derived stem cells from the adult mouse cornea. *Stem Cells* **24**, 2714–2722.
4 Du Y, Funderburgh ML, Mann MM, SundarRaj N, Funderburgh JL (2005) Multipotent stem cells in human corneal stroma. *Stem Cells* **23**, 1266–1275.
5 Davanger M, Evensen A (1971) Role of the pericorneal papillary structure in renewal of corneal epithelium. *Nature* **229**, 560–561.
6 Funderburgh ML, Du Y, Mann MM, SundarRaj N, Funderburgh JL (2005) PAX6 expression identifies progenitor cells for corneal keratocytes. *FASEB J.* **19**, 1371–1373.
7 Limb GA, Daniels JT (2008) Ocular regeneration by stem cells: present status and future prospects. *Br. Med. Bull.* **85**, 47–61.
8 Lwigale PY, Cressy PA, Bronner-Fraser M (2005) Corneal keratocytes retain neural crest progenitor cell properties. *Dev. Biol.* **288**, 284–293.
9 Whikehart DR, Parikh CH, Vaughn AV, Mishler K, Edelhauser HF (2005) Evidence suggesting the existence of stem cells for the human corneal endothelium. *Mol. Vis.* **11**, 816–824.
10 Takacs L, Toth E, Berta A, Vereb G (2009) Stem cells of the adult cornea: from cytometric markers to therapeutic applications. *Cytometry A* **75**, 54–66.
11 Brandl C, Florian C, Driemel O, Weber BH, Morsczeck C (2009) Identification of neural crest-derived stem cell-like cells from the corneal limbus of juvenile mice. *Exp. Eye Res.* **89**, 209–217.
12 Winer J, Jung CK, Shackel I, Williams PM (1999) Development and validation of real-time quantitative reverse transcriptase-polymerase chain reaction for monitoring gene expression in cardiac myocytes in vitro. *Anal. Biochem.* **270**, 41–49.
13 Sarthy VP, Brodjian SJ, Dutt K, Kennedy BN, French RP, Crabb JW (1998) Establishment and characterization of a retinal Muller cell line. *Invest. Ophthalmol. Vis. Sci.* **39**, 212–216.
14 Rao CV, Yamada HY, Yao Y, Dai W (2009) Enhanced genomic instabilities caused by deregulated microtubule dynamics and chromosome segregation: a perspective from genetic studies in mice. *Carcinogenesis* **30**, 1469–1474.
15 Tomas-Loba A, Flores I, Fernandez-Marcos PJ, Cayuela ML, Maraver A, Tejera A *et al.* (2008) Telomerase reverse transcriptase delays aging in cancer-resistant mice. *Cell* **135**, 609–622.
16 Flores I, Benetti R, Blasco MA (2006) Telomerase regulation and stem cell behaviour. *Curr. Opin. Cell Biol.* **18**, 254–260.
17 Samper E, Flores JM, Blasco MA (2001) Restoration of telomerase activity rescues chromosomal instability and premature aging in Terc−/− mice with short telomeres. *EMBO Rep.* **2**, 800–807.
18 Krishnamurthy J, Ramsey MR, Ligon KL, Torrice C, Koh A, Bonner-Weir S *et al.* (2006) p16INK4a induces an age-dependent decline in islet regenerative potential. *Nature* **443**, 453–457.
19 Sharpless NE, Bardeesy N, Lee KH, Carrasco D, Castrillon DH, Aguirre AJ *et al.* (2001) Loss of p16Ink4a with retention of p19Arf predisposes mice to tumorigenesis. *Nature* **413**, 86–91.
20 Gartel AL, Radhakrishnan SK (2005) Lost in transcription: p21 repression, mechanisms, and consequences. *Cancer Res.* **65**, 3980–3985.
21 Gartel AL, Serfas MS, Tyner AL (1996) p21–negative regulator of the cell cycle. *Proc. Soc. Exp. Biol. Med.* **213**, 138–149.
22 Martin-Caballero J, Flores JM, Garcia-Palencia P, Serrano M (2001) Tumor susceptibility of p21(Waf1/Cip1)-deficient mice. *Cancer Res.* **61**, 6234–6238.